Feline Wolf Net: A Hybrid Lion-Grey Wolf Optimization Deep Learning Model for Ovarian Cancer Detection

Dr. Moresh Mukhedkar[1], Divya Rohatgi[2], Dr. Veera Ankalu Vuyyuru[3], Dr K V S S Ramakrishna[4], Prof. Ts. Dr. Yousef A.Baker El-Ebiary[5], Dr.V.Antony Asir Daniel, M.B.A., M.E., Ph.D[6]
Assistant Professor, D Y PATIL UNIVERSITY, Pune, India[1]
Dept. of CSE-ASET, Amity University, Maharashtra, India[2]
Assistant Professor, Department of Computer Science and Engineering, Koneru Lakshmaiah Education Foundation, Vaddeswaram, 522502, A.P, India[3]
Department of CSE, Vignan's Nirula Institute of Technology and Science for Women, Pedapalakaluru, Guntur-522005, Andhra Pradesh, India[4]
Faculty of Informatics and Computing, UniSZA University, Malaysia[5]
Associate Professor and Head of the Department, Department of Electronics and Communication Engineering, Loyola Institute of Technology & Science, Kanyakumari-629302, Tamilnadu, India[6]

***Abstract*—Ovarian cancer is a major cause of mortality among gynecological malignancies, emphasizing the critical role of early detection in improving patient outcomes. This paper presents an automated computer-aided design system that combines deep learning techniques with an optimization mechanism for accurate ovarian cancer detection that utilizes pelvic CT images dataset. The key contribution of this work is the development of an optimized Bi-directional Long Short-Term Memory (Bi-LSTM) model which is introduced in the layers of CNN (Convolutional Neural Network), enhancing the learning process. Additionally, a feature selection method based on Lion with Grey Wolf Optimization (LGWO) is employed to enhance classifier efficiency and accuracy. The proposed approach classifies ovarian tumors as benign or malignant using the Bi-LSTM model, evaluated on the Ovarian Cancer University of Kaggle dataset. Results showcase the effectiveness of the method, achieving remarkable performance metrics, including 98% accuracy, 99.7% recall, 93% precision, and an impressive F1 score of 98%. The proposed method's efficiency is validated through comparison with validating data, demonstrating consistent and reliable results. The study's significance lies in its potential to provide an accurate and efficient solution for early ovarian cancer detection. By leveraging deep learning and optimization, the proposed method outperforms existing approaches, highlighting the promise of advanced computational techniques in improving healthcare outcomes. The findings contribute to the field of ovarian cancer detection, emphasizing the value of integrating cutting-edge technologies for effective medical diagnosis.**

Keywords*—Ovarian cancer; deep learning; bidirectional long short term memory; CT images; convolutional neural network; lion grey wolf optimization

I. INTRODUCTION

Ovarian cancer is the occurrence of irregular cells in the ovary which reproduce uncontrollably and then causes tumor malignancy in the tissues [1]. This can be categorized into three major types namely sex-cord- stromal, epithelial and germ cell. In this epithelial ovarian cancer has a secondary type namely clear cell, mucinous, serous and endometriosis. Serous tumors are segregated into low-grade serious carcinomas (LGSC) and high-grade serous carcinomas (HGSC). By analysis it shows that 70-80% people cause epithelial cancer, clear cell in addiction with mucinous are induced to less than 5% people and 10% people cause endometriosis. The first sign of ovarian cancer is epithelial cancer, which must be detected early to prevent death. Ovarian cancer should be detected in early stage, for detecting involves various methods and this paper proposed the ovarian cancer through deep learning [2]. Epithelial ovarian cancer made up of diverse ancient subsets with peculiar genomic features, they are enhancing the accuracy and effectiveness of healing treatment. It enables the detection of reaction such as ovarian cancer susceptibility genes BRCA2 and BRCA1 and also corresponded combining deficiency with damage in DNA response pathway resistance either inhibitor. This procedure is to process genomic transformation in tumors along with blood to evaluate sensitivity, therapy resistance and precise residual disease indicator. Around 230000 women shall be analyzed and 150000 women are died. This signifies that EOC is the seventh usually detected cancer in women. Genetic syndromes comprise Peutz-Jegher along with uncommon disorders and they are nevoid basal cell sign. Their causative factor includes an embryonic pregnancy, initial menarche, fallen age menopause, smoking, polycystic ovary syndrome [3].

Ovarian cancers are predicted by two medical examinations they are serum cancer antigen 125(CA125) and transvaginal ultrasound. Specificity along with sensitivity is restrictions. CA125 is frequently raised in benign stage including endometriosis and ovarian cysts. It is not determined in initial stage. This test evaluates the quantity of protein named CA-125 within the blood. High stages of CA-125 are occurred in women. This test is beneficial as tumor marker to identify as ovarian cancer. High level of CA125 persons fails

to validate ovarian cancer because it might be endometriosis and pelvic inflammatory disease. Person with abnormal CA-125 level, medical practitioner again examines the report. CA-125 is widespread in countries such as Canada, Australia, United States and Ireland as an prediction for ovarian cancer [4]. Transvaginal Ultrasound (TVUS) is a checkup that utilizes sound waves to monitor the uterus, fallopian tubes and ovaries by fixing ultrasound wand inside the vagina. It detects massive tumor or benign take placed [5]. The most present worldwide statistic calculates 295,414 recently predicted cases of ovarian cancer all year and also this disease causes 184799 yearly dead. Moreover, in an advanced phase 75% of ovarian cancer patients are difficult to diagnose properly. The treatment of chemo resistant ovarian cancer by targeting mitochondria has observed. It is developed under the terms where cancer cells modify and swap to mitochondrial respiration this turns severe to endurance so that perfect metabolic focus for chemo resistant ovarian cancer. In ovarian cancer tumor metastasis together with chemoresistance are allied in mitochondria spatial redistribution. Aberrant dependence of mitochondrial pathways are caused by specific sets of genetic mutation [6].

Recent treatment strategies include by combining debulking surgery, radiation therapy and drug treatment. Some sophisticated remedies are immunotherapy, hormone therapy and targeted therapy. OC treatment mainly involves chemotherapy. Repeatedly applied chemotherapeutic agents employed for curing of ovarian cancer includes platinum comprising drugs i.e., carboplatin along with cisplatin and tisane family i.e., docetaxel together with paclitaxel. In recent days, scientists have been providing an immunotherapy approach to treat gynecologic cancers. From ascites, tumor and blood of ovarian cancer patients the T cells and Antibodies are predicted in immunotherapy [7]. The machine learning algorithms are involved in several data mining applications which include ovarian cancer. Although these algorithms don't perform suitably due to inaccurate computational complexity, data imbalance, and missing values. Recently deep learning-based process has gained advantage in computer vision related applications and data mining over machine learning. Deep Learning Network utilized in several regions such as speech recognition, computer vision, healthcare, image processing [8]. In this research, emphasize on developing a deep learning established system for classification of ovarian cancer. The systematic study highlights the Bi-LSTM classifier which effectively worked and maintained more accuracy than other classifier such us CNN, 3D-CNN, KNN and Random Forest classifier. The deep learning handles the data by various phases including convolution layer, dense layer and pooling layer. Commonly deep learning have sequential architecture pursued by feature extraction, feature selection and classification [9]. Deep learning is frequently used invading detection of ovarian cancer. Deep learning scheme Bi-LSTM network performs a vital function to enhance the classification [10]. Optimization algorithms can be used to automatically identify and extract important features from the data in the image especially size, shape, and area of the tumor occur in ovary. This helps to remit the time required and potential for manual analysis, and can also develop the accuracy of the detection process. Optimization algorithms can also be used to train deep learning models that can automatically classify medical data as either containing a tumor or not. These models can be optimized to improve their performance, such as by adjusting their parameters or optimizing their training process.

The key contribution of the described outline is given as follows:

- The development of an optimized Bi-LSTM model for the early detection of ovarian cancer.
- The novelty of this work lies in the development of an optimized Bi-LSTM model for ovarian cancer detection, which enhances the learning process and achieves impressive performance metrics.
- By utilizing deep learning techniques and an optimization mechanism, this model enhances the learning process and improves the accuracy of classification.
- Additionally, a feature selection method called Lion with Grey Wolf Optimization (LGWO) is employed to further enhance the efficiency and effectiveness of the classifiers.
- The combination of the Bi-LSTM model and the LGWO feature selection method allows the system to accurately classify ovarian tumors as either benign or malignant.
- To validate the efficiency and reliability of planned method, its presentation metrics are compared with the validating data, demonstrating consistent and reliable results.

The configuration of this essay is as accompanies: Section II contains the related work that is framed to understand the proposed paper with the existing methods while Section III elaborates the problem statement. Section IV depicts the proposed LGWO-Bi-LSTM architectures. The results and performance metrics are tabulated and graphically represented in Section V. Finally, in Section VI, conclusion and future works are presented.

II. Related Work

Srivastava et al. [11] outlined adjusted VGG-16 deep learning, ovarian cyst detection was accomplished approach. Pretrained deep learning method consists of VGG-16 model. To understand the VGG-16 model keenly a multiple of 3×3 kernel sized filters are obtained. This explains the established VGG-16 prototype fine- tuned with the data-set of ultrasonic images. Modifying the VGG-16 model's top four layers allows for fine-tuning. Distinct women's sample ovarian images are gathered to detect if ovarian cyst is occurred or not. The accuracy of 92.11% is obtained. The downside of VGG-16 deep learning network is slower than the ResNet architecture. Meng et al. [12] Intended virtual historical method of staining with deep generative adversarial mechanism to determine the ovarian cancer. Here hematoxylin and also Eosin staining method are used. Depending upon GAN, here autofluorescence images are created to develop a weakly supervised learning method of unstained ovarian tissue

regions depending upon E and H staining portion of ovarian tissues. The characteristic of the result predicted by the approach is more precise. This paper proposed a valid autofluorescence image generation of algorithm in the insufficient data which can consume time and laborious data representations in many situations. Through doctors determined the accurate unstained fluorescence image of ovarian cancer can be generated by this mechanism is 93%. The existing algorithm involves several complexities to predict the ovarian cancer. The visual evaluation established through deep learning method reaches an accuracy of 95%. Lu et al.[13] Proposed the determination of ovarian cancer by machine learning. It detects the exact of benign and ovarian tumors. In this method includes several processes like blood test, demographics, tumor markers and general chemistry. 349 Chinese individuals' information regarding 49 characteristics were obtained, and 235 patients' data were processed using the machine learning Minimum Redundancy - Highest Relevancy approach. The MRMR adopts 10 noteworthy characteristics, including human epididymis protein 4 (HE4) and cancer-embryonic antigen (CEA) are top featured by the decision tree model. It shows that machine learning is mostly incredible in detecting the complex diseases. The accuracy of trained data of ROMA, Decision Tree, and Logistic Regression is 79.6%, 87.2%, 84.7% and the accuracy of test data of ROMA, Decision Tree, and Logistic Regression is 92.1%, 95.6%, 97.4% respectively. This method is largely unstable contrasted with the other decision approaches. Schwartz et al.[14] Proposed an automated structure to recognize ovarian cancer in transgenic mice through optical coherence tomography (OCT) recordings. Classification is achieved by a neutral network that distinguishes structurally ordered sequence of tomograms. It consists of three neural networks they are 3D convolutional neural network, VGG-supported feed-forward network and convolutional long short-term memory network. The outcome indicates that it can accurately output manual tuning although there is a default in noise inherent OCT images. It obtained a mean of 0.81± 0.037.

Yang et al. [15] Proposed the detection of ovarian cancer by combining the clinical significance of salivary mRNAs together with carcinoembryonic antigen. It is a liquid biopsy method and it can be used to predict many types of cancers. Here we determined a discriminatory study of ovarian cancer by uniting CEA and salivary mRNA biomarkers. Using two methods this technique is achieved. They are independent validation phase and discovery phase in which finding and evaluating of multiple biomarkers is enabled by discovery phase, independent validation phase confirms the availability of the finest bio-markers. Discovery phase categories blood's CEA level and five mRNA biomarkers in saliva are noted. Novel panel of biomarkers is used to segregate ovarian cancer patients and healthy people with high specificity of 82.9% and also with high sensitivity of 89.3% are obtained. In validation phase it acquires sensitivity 85% and simplicity 88.3%. Lemmings et al. The author in [6] proposed the treatment of chemo resistant ovarian cancer by targeting mitochondria. It is developed under the terms where cancer cells modify and swap to mitochondrial respiration this turns severe to endurance so that perfect metabolic focus for chemo resistant ovarian cancer. In ovarian cancer tumor metastasis together with chemoresistance are allied in mitochondria spatial redistribution. Zhang et al. [16] For manufacturers to offer more advanced and inexpensive, high-quality Ultrasonic Flaw (UT) technology that could improve maternity medical services, it is recommended that we tackle the requirement to establish sustained sonar criteria with tolerably high pregnant and neonatal death rates. A group of artificial intelligence techniques, like the most recent advances in training to learning for maternal ultrasonography, is growing in acceptance and sparking excitement across a number of industries, such processing images for artificial intelligence. In this study, sophisticated artificial intelligence (AI) algorithms that use logistic reconstruction classifiers (LRC) and convolution neural networks (CNNs) to associate the original input picture to the intended outcome image are of special interest. Additionally, they employed the Internet of Medical Things (IoMT) to divide up maternal tumour imaging and identify tumours for specialists. The experimental findings demonstrate that the LRC based on CNN may be utilised for predicting the outcomes of maternity ultrasounds with enhanced levels of paternal and neonatal movement.

Kaggie et al. [17] proposed Ovarian cancer is one of several tumour subgroups that may be characterized using multipara metric magnetic resonance imaging (MRI). Despite the limitations of traditional anecdotal T1- and T2-weighted scans, quantified mappings of MRI relaxation values, including T1 and T2 the mapping process, shows promise for improved tumour evaluation. Nevertheless, due to the ordered measurement of several parameters, quantitative MRI relaxation mapping approaches sometimes need lengthy scan periods. Fast qualitative MRI is made possible by a novel technique called magnetic resonance fingerprinting (MRF), which takes use of transitory signals brought on by changes in the parameters that make up of a pseudorandom programme. Statistical corresponds are subsequently created by matching these temporary signals to a computed lexicon of T1 and T2 elements. The capacity of the MRF to monitor several factors concurrently may provide a novel method for identifying malignancy and evaluating the effectiveness of treatments. Using ovarian cancer as an illustration structure, this practical research examines MRF for concurrent T1, T2, and relative proton density (rPD) mapping. Negi et al. [18] proposed In comparison to monolayer OLED design, a unique three hole block layer (HBL) arrangement of the OLED is presented that exhibits improved luminosity of 25285 cd/m2. The 74% increase in illumination power efficiency is partly to blame. The internal circuit evaluation is used to confirm an extensive numerical analysis built on the Poisson and drift dispersion model. The results of the examination show that the suggested gadget has a higher rate of recombine. A higher amount of recombination is a result of effective whole shielding as well as elevated particle input. Consequently, ovarian cancer is diagnosed by triple HBL OLED. The gadget produced an ultimate photon current level of 93 mA and had good responsiveness to different bands. According on their urine's ability to shine, a healthy individual can be distinguished from an oncological cancer survivor.

III. PROBLEM STATEMENT

The detection of ovarian cancer is crucial for preventing patient mortality. However, there are several challenges associated with this process, such as the risk of infection, bleeding, blood clot formation, swollen legs, fatigue, infertility, and bowel changes. To aid in the detection process, a fine-tuned VGG-16 model has been developed to categorize ovarian cysts based on their forms, cysts, HOC, dermoid cysts, and PCOS. However, the current system lacks a user interface that allows pathologists to conveniently upload and predict images, which needs to be addressed and improved [19]. The fine-tuned VGG deep learning network more time to train its parameters [11].

IV. PROPOSED LGWO-BASED BI-LSTM

Initially the ovarian cancer dataset is preprocessed through weaned filter and then image segmentation is employed by Fuzzy C-means clustering. In this way feature is extracted using Grey Level Co-occurrence Matrix and feature is adopted by hybrid Lion Grey Wolf optimization and also categorized by Bi-LSTM model. Block diagram of hybrid Lion Grey Wolf Optimization through Bi-LSTM model is depicted in Fig. 1.

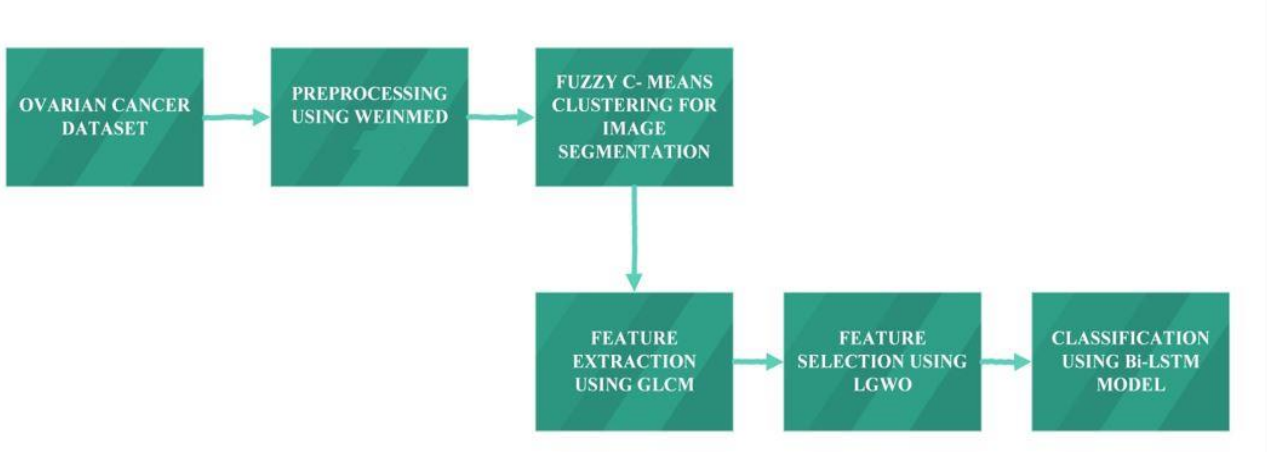

Fig. 1. Block diagram of hybrid lion grey wolf optimization through Bi-LSTM model.

A. Data Collection

The research utilizes pelvic CT image datasets affiliated with China's Qingdao University, specifically from a Class 3 hospital. After screening the obscured data, it acquired a totality of about of 5100 CT images of 223 patients containing pelvic CT images with highlights were gathered and utilized. The images were divided into two equal sets, with 50% used as training data and the other 50% used as testing data. This means that 2550 images with highlights were utilized for training and 2550 CT images with highlights were utilized for testing. The dataset consists of 2000 pelvic CT images collected from 223 patients. It contains three types of pelvic CT images containing clear cell, mucinous, endometriosis and serous. Pelvic CT images taken for mucinous, clear cell and endometriosis is 2000, 1500, and 1600 for ovarian cancer [20].

B. Pre-processed by Weinmed Filter

The most crucial stage for the best categorization outcomes is pre-processing. It is frequently carried out on data before classification to make sure the desired outcomes are reached [21]. The CT images that obtained are pre-processed to get more relevant for further process. The preprocessing step includes smoothing, toughen the edges of the image and noise removal. The objective of pre-processing enhances the image quality. Each pixel replaced weinmed filter with average value of intensities in region. Median filter removes salt and noise accurately. Weinmed filter probes to construct an optimal determination of the original image by enforcing the minimum mean square error limit between estimate and original image. The purpose of the weinmed filter is to reduce the mean square error and it also de-blurs the image and reverses filtering. This filter also opens morphological operation and contrast enhancement to image enhancement and reduce noise. Individual background noises calculate the contrast of each region. By preserving the edge information of unclear areas, the background noise is removed shall highlights the digital prototype. Both the degradation function and noise are managed by weinmed filter. Through the degradation model, the error among the estimated signal and the input signal is provided.

Weiner filter formula is expressed in Eq. (1),

$$F_{X(u,v)}=\frac{|H(u,v)|^2}{|H(u,v)|^2+S\frac{P_{n(u,v)}}{P_{f(u,v)}}}\,G(u,v)*\frac{1}{H(u,v)} \quad (1)$$

$\boldsymbol{P_{n(u,v)}}$ - Noise power spectrum

$\boldsymbol{P_{f(u,v)}}$ - Power Spectrum of the original image

H (u, v) –Fourier Transform of the point spread function

G (u, v) –Power Spectrum with the Fourier change of the noisy point cloud image

$\boldsymbol{F_{X(u,v)}}$ -Result Value After restoration

The computed de-noising equation is given below.

Let FUV stand for the collection image parameters in a k-by-1-inch square sub image windows centered at the two points (u, v). The following phase in preparation is to remove and normalize the surrounding data during processing itself, albeit this might affect the results of segmentation. During this

moment, the edge from the CT ovarian equation is identified using a clever edge detecting approach Eq. (2) [22].

$$f(u,v) = Median\{F_{X(u,v)}\} \in Fu,v \quad (2)$$

The above equation (2) is termed as Weinmed filter.

C. Segmentation using Fuzzy C-means Clustering

The segmentation process involves identifying and labeling the different regions in the CT images, such as the mucinous, clear cell, endometriosis, and serous. This task can be challenging due to the complex and heterogeneous nature of ovarian cancer, which can exhibit variations in size, shape, location, and intensity. In addition, there can be variability in the imaging protocols and noise artifacts that can affect the quality of the images. Segmentation of ovarian cancer using CT images can be performed using a variety of techniques, such as threshold, region-growing, active contours, and machine learning-based approaches. Here, Fuzzy clustering method is adopted to perform the task. In the context of ovarian cancer detection, image segmentation using fuzzy clustering can be used to separate the tumor region from the ovarian cancer. The segmentation result can then be used for quantitative analysis and clinical decision-making. Several studies have reported promising results using fuzzy clustering for ovarian cancer segmentation.

Fuzzy C-means clustering is preferable optimization for feature segmenting the CT images. It is the most common fuzzy algorithm which is extremely delicate to outliers, noise, and size of the clusters. It starts by randomly initializing the cluster centroids and the fuzziness parameter, and then iteratively updates the centroids and the degree of membership until convergence. The segmentation result is obtained by assigning each pixel to cluster with highest degree of membership. After initializing degree of membership values, the cluster centroids are calculated and then according on how far there is among every point of data to the geographic center of every cluster, the range of membership metrics associated with each observation point was modified. The levels of values for membership have been updated the cluster centers are re-computed using the weighted average of the data points. Repeat the process until convergence. Once, the algorithm converges, the final assignment of each data point to a cluster is based on the highest degree of membership value [23].

Let us consider a number of finite dataset be 'n' and A = $(a_1, a_2, \ldots, a_n)$. The dataset A is divided in to group of cluster by using FCM algorithm. Formula for FCM algorithm is given in Eq. (3).

$$J_s = \sum_{p=1}^{n}\sum_{q=1}^{c} u_{pq}^{s} \left\|A_p - C_q\right\|^2 \quad (3)$$

Where, $u_{pq} = \frac{1}{\sum_{k=1}^{c}\left(\frac{d_{pq}}{d_{kq}^{*}}\right)^{\frac{2}{s-1}}}$ is the degree of membership value of x_p in q^{th} cluster, x_p is p^{th} data points and $c_q = \frac{\sum_{q=1}^{n} u_{pq}^{s}}{\sum_{q=1}^{n} u_{pq}^{s}} x_p$ is q^{th} cluster center, s denotes the fuzzy parameter and Euclidean distance is represented as‖ ‖ .

Where, d_{pq} indicates the aloofness among data points x_p and q^{th} cluster focus and d_{kq}^{*} is distance between k^{th} cluster focus and q^{th} cluster center.

D. Feature Extraction using Scale-Invariant Feature Transform (SIFT)

Finding the initial corresponding characteristics is the aim of the initial phase. The starting imagery A and those perceived image B, both of whom are fed to SIFT to extract and characterize local characteristics, are two separate images that need to be registered F_A and F_B, accordingly.

The prospective features are found by scanning across all of the available sizes and places of residence for extracted features. The regional maximal and minimal values of E(x), which can be described as the combination of the function using an image, i.e., F_A or F_B, are used to discover scale-space extreme. Another thorough match to the neighboring data points is carried out to determine the precise positions of the characteristics [24]. Some prospective feature points have inadequate contrast elements or edge locations with poor localization, thus the contrasting values and primary curved proportions are utilized to exclude the unstable characteristics. After reliable prospective characteristics are discovered, every key point is given a dominant orientations determined by the current picture gradients directions histogram to achieve image rotational consistency [25]. A description matrix that is calculated for every distinctive point comes next. A 3-D histogram of grade dimensions and directions serves as such a description. To create a 128-D descriptor, the gradients alignment angle is compressed into eight orientations increments and the placement is compressed into a 4 4 placement grid.

$$\theta = \cos^{-1}\left(\frac{Z_p^{H} Y_p}{\left\|Z_p\right\|\left\|Y_p\right\|}\right) \quad (4)$$

where, Z_p represents the p th feature descriptors vector in that the sensed imagery, Y_p represents the p th feature descriptor vector in the reference image, and represents the angle among the two variables. The primary maximum degree versus the second minimum angle ratio, represented by the symbol proportion, is utilized to increase the accuracy of matching the initial characteristics. Initial match characteristics are disregarded if their angle ratios of distance are higher than a threshold value.

The combination of entropy together with the mean value of Fourier co-efficient is obtained to provide feature vector in AGLCM algorithm.

E. Feature Selection using Hybrid LGWO

The Lion with Grey Wolf Optimization algorithm is employed to reducing the errors in training data and detects the malignant portion. Here the leader may be male or female indicated as alpha which enables hunting, sleeping, time to wake, location. Alpha makes decision and Beta handles.

Omega is the lower section of the grey wolf and for further wolves on every occasion [26]. Omega (ω) is noticed as the leftover provision [27]. In Lion optimization the parameters include learning rate (α), weight values (w), number of layers (L), kernel sizes (k) and dropout rate (γ).

1) Initialization process: At first the preprocessed output data is initialized as a, B and C as coefficient vectors.

Fitness evaluation:

Eq. (5) evaluates the fitness utility and predicts the result

$$Fit_i = \max accuracy \tag{5}$$

Differentiate the solution depend on filters:

Let the initial fitness bed_α, the second finest fitness be d_β, the third finest fitness be d_δ

a) Roaming: In this process the territory is visited by every male lion where the total location to number of this location is %S. When the Lion find the best location it reforms the location during roaming. Lion shifts to improved location is denoted in Eq. (6) [28]

$$\gamma \sim U(0,2) \times g \tag{6}$$

Where, g – Male lion' current location and selected location from the territory and *U* – Uniform Distribution

$P_{si} = 0.1 + min\left(0.5, \frac{(Y_i - Y_{best})}{Y}\right)$, i=1, 2, 3 …no. of nomad lions

Where, $P_{si} =$ the chance detected for seperation of all nomad lions $Y_i = i_{th}$ Lion's fitness value and $Y_{best} =$ Fitness value of the best nomad lion.

b) Encircling prey: Together with these three contenders by α, β, δ and also ω. In addiction for the group to track a prey is by surrounding their location. Encircling or trapping behaviour of grey wolves for pray during hunting is computed using the following Eq. (7) and (8) [29].

$$d(t+1) = d_{ps}(t) = \vec{B}.\vec{K} \tag{7}$$

$$\vec{K} = \left|\vec{C}.d_{ps}(t+1) - d_{ps}(t)\right| \tag{8}$$

Where, $\vec{B} = 2\vec{c}r_1 - \vec{c}$ and $\vec{C} = 2r_2$, and $d_{ps}\ (t)$ - The prey position, *B and C* – The coefficient vector, $\vec{c}$ - Linearly lowered from 2 to 0, $r_1 and r_2$- Random vector[0,1], and *t* - The iteration n numbers.

c) Hunting: Hunting is done based upon Lion Optimization. In every pride the female concentrates on a prey in a cluster to feed their pride. To surround the victim and to preserve pride it follows certain mechanisms. All lions fine-tuned their localities to rely on particular locality and the group associates' localities. Due to this reason the seekers surround the victim and apply relative training, assaults from locality conflict. For this the seekers are classified into three subdivisions. In the centroid of seekers, a prey is engaged. During hunting the hunters are chooses in sequence, a false victim is assaulted by decided seekers in order with the crowd which decides lion to belong it. If a searcher enhances its fitness a false victim escape from searcher and new locality of prey is detected in Eq. (9) [30].

$$d_{ps}{}' = p + ran(0,1) \times PI \times (p - h) \tag{9}$$

Hunter represents the present locality seeker who hit to victim and PI denotes the objective seekers increasing rate in Eq. (10).

$$h' = \begin{Bmatrix} rand\big((2 \times p - h), p\big)\ if\ (2 \times p - h) < ps \\ rand\big(p, (2 \times p - h)\big)\ if\ (2 \times p - h) > ps \end{Bmatrix} \tag{10}$$

The new localities of centroid seekers are given bin Eq. (11)

$$h' = \begin{Bmatrix} rand(h, p)\ if\ (2 \times p - h) < ps \\ rand(p, h)\ if\ (2 \times p - h) > ps \end{Bmatrix} \tag{11}$$

The above equation produces an arbitrary value from b to c which is upper and lower limits, respectively.

Understanding and improving the effectiveness of the suggested model depends on research into how the HLGWO's characteristics affect the identification of ovarian cancer. These parameters include a wide range of factors, including population size, convergence standards, crossover and mutation rates, and trade-offs between exploitation and exploration. It is feasible to fine-tune the HLGWO algorithm to increase its efficiency and efficacy in optimizing the deep learning model for ovarian cancer diagnosis by carefully modifying and analyzing these parameters. The model's convergence rate and solution quality can be considerably impacted by striking the correct balance between exploration and exploitation. Additionally, preventing premature convergence and finding the most illuminating characteristics for precise identification may be achieved by optimizing parameters like mutation rates and crossover rates. To further improve HLGWO's potential as a diagnostic tool for ovarian cancer, it is crucial to refine and adapt the model for practical clinical applications. This requires understanding how these parameter adjustments influence the model's sensitivity, specificity, and overall accuracy.

F. Classification using Bi-LSTM

Classifications of RNN include Bi-LSTM it is enabled for processing of natural language like text classification. The context is captured as it is a powerful model and words depend on sequence [31]. In ovarian cancer classification, Bi-LSTM networks can be used to predict sequences of MRI or CT scans to classify ovarian cancer as benign or malignant. The input sequence can consist of images from different angles, slices, and time points and the network can learn to recognize patterns and features that are indicative of specific ovarian cancer types. Bi-LSTM model is represented in Fig. 2. In addition, Bi-LSTM networks can also be concatenated with other DL techniques, such as CNNs, to enhance the accuracy of the classification. Convolution neural networks are commonly used to extract data from medical images, while Bi-LSTM networks can learn the temporal dependencies between these features. Overall, Bi-LSTM networks are a promising tool for brain tumor classification because they can model the complex relationships and patterns in sequential

data, thus improving the accuracy of classification by utilizing backward hidden states, which contributes to the enhancement of LSTM network learning [32].

Four gates in LSTM neural network are represented in Eq. (12) to (15).

$$c_t = \sigma(M_f x_t + E_f h_{t-1} + c_c) \quad (12)$$

$$d_t = tanh(M_g x_t + E_g h_{t-1} + c_d) \quad (13)$$

$$e_t = \sigma(M_i x_t + E_o h_{t-1} + c_e) \quad (14)$$

$$f_t = \sigma(M_o x_t + E_o h_{t-1} + c_f) \quad (15)$$

where, Ef, Eg, Ei, Eo represents the weight matrices of the preceding short-term state ht-1. Mf, Mg, Mi, Mo represents the weight matrices of the present input state xt, and cd, ce, cf, and co are the bias terms. Where, p_{t-1} represents the previous long-term state.

The present long-term state of the network g_t can be evaluated by using Eq. (16), and y_t can be evaluated using Eq. (17).

$$g_t = f_t * p_{t-1} + e_t * d_t \quad (16)$$

$$y_t = h_t = f_t * \tanh(g_t) \quad (17)$$

The classification architecture is depicted in below by given Fig. 2. Similar to this, the LSTM layer gains knowledge of the dependencies among various time steps in sequence data.

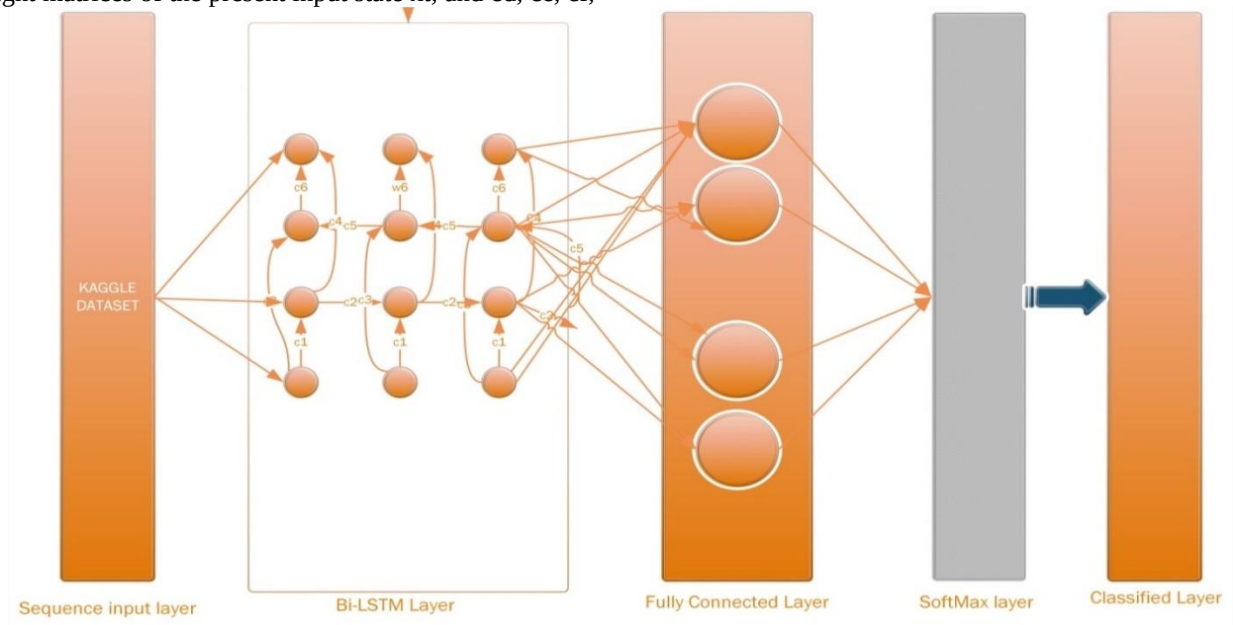

Fig. 2. Bi-LSTM classification of architecture.

Algorithm 1: LGWO- Bi-LSTM mechanism

INPUT: *CT images from Kaggle dataset*
OUTPUT: *Classifying the type of ovarian cancer (clear cell, mucinous, serous and endometriosis)*
Load input image data
C$=\{c_1, c_2, c_3, \ldots . c_n\}$ *//Image acquisition*
Pre-processing of images
Toughen the edges of the image *//Weiner filter*
Removes the salt and noise effectively *//Median filter*
Segmentation of images
Choose the initial cluster and membership matrix *//Fuzzy C-means Clustering*
Calculate new cluster and new membership matrix
If (Difference in cluster center)
< threshold
Stop
Else
>threshold
Repeat
Feature Extraction
Feature Selection *//LGWO*
Calculate roaming using the fitness of Lion
Calculate encircling using the fitness of Grey Wolf
Calculate hunting using the fitness of Lion
Classification *//Bi-LSTM*

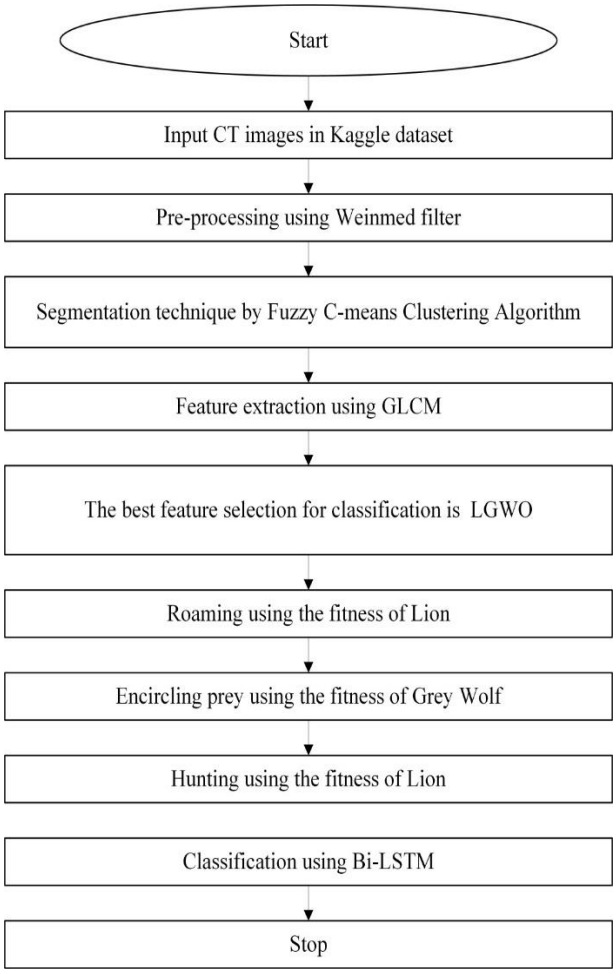

Fig. 3. Flow diagram of HLGWO -BI-LSTM model.

The above Fig. 3 elaborates the overall work flow of the entire proposed model. Main steps involved in detecting and classifying the ovarian cancer shown in flow with algorithmic conditions. This flow chart helps for quick understanding of the presented research.

V. Result and Discussion

This study provides a detailed explanation of the experimental results obtained from the proposed method, using numerical terms to quantify the outcomes. The validation process was conducted on the CT images. The Kaggle dataset comprising 223 patient's datasets containing 5100 CT images were separated 50% as testing along with training data. The proposed system's evaluation was compared with three classification methods: ML-CNN, HOG-ANN, and UBOC. Performance evaluation of the Bi-LSTM classifier and LGW optimization algorithm is carried out using four metrics such as accuracy, F1 score, precision, recall. Entire experimental process is implemented by using MATLAB software in windows 10 platform.

A. Evaluation of Performance Metrics

The experiment assessed the models using four evaluation metrics: accuracy, F1-score, precision, and recall. These parameters are specifically defined in Eq. (18) to (21).

$$Accuracy = \frac{TP+TN}{TP+TN+FP+FN} \quad (18)$$

$$Recall = \frac{TP}{TP+FN} \quad (19)$$

$$Precision = \frac{TP}{TP+FP} \quad (20)$$

$$F1score = \frac{2*Recall*Precision}{Recall+precision} \quad (21)$$

In above equations, TP refers to the no. of data finely classified as positive out of all the data that were actually positive. TN Refers to the no. of data finely classified as negative out of all the data that were actually negative. FN is the number of data that were mistakenly classified as negative by the model even though they were actually positive in the dataset. FP is the number of data that were mistakenly classified as positive by the model even though they were actually negative in the dataset, Recall is defined as the ratio of the no. of data classified as positive by the model to the actual no. of data that were positive in the dataset. Precision is the ratio between no. of data that were correctly classified as positive by the model and the total no. of data defines positive. Finally, F1-score is the harmonic mean of recall and precision, as explained in [33].

TABLE I. Experimental Result Analysis for Different Parameters with other Metrics

Method	Accuracy	Recall	Precision	F1-score
ML-CNN[34]	96.5	96	98	97
CNN-DenseNet[35]	94.73	98.9	91	95
AlexNet[36]	84.45	90	75	87
Proposed Bi-LSTM-LGWO	98	99.7	93	98

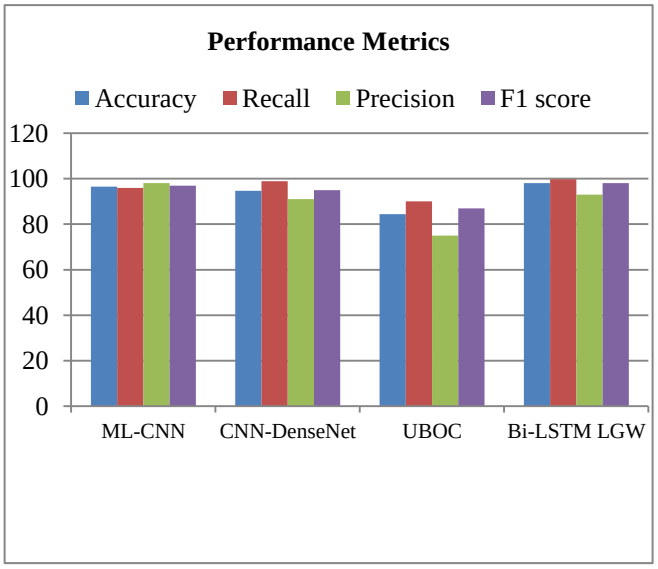

Fig. 4. Performance evaluation of various methods of classification.

In Table I, the performance evaluation of the proposed system is tabulated. The proposed Bi-LSTM-FFO shows higher accuracy when compared with other classifiers. Average of Precision and recall of the existing methods is higher than the proposed method. Mean value of precision

and recall gives a significant measure of classification called F1-score; the graphical identification of performance analysis is shown in Fig. 4.

TABLE II. COMPARED RESULT IN TERMS OF SENSITIVITY AND SPECIFICITY

Method	Specificity	Sensitivity
ML-CNN[34]	89.7	90.57
CNN-DenseNet[35]	96.94	95
AlexNet[36]	95	72
Proposed Bi-LSTM-LGWO	96.4	98

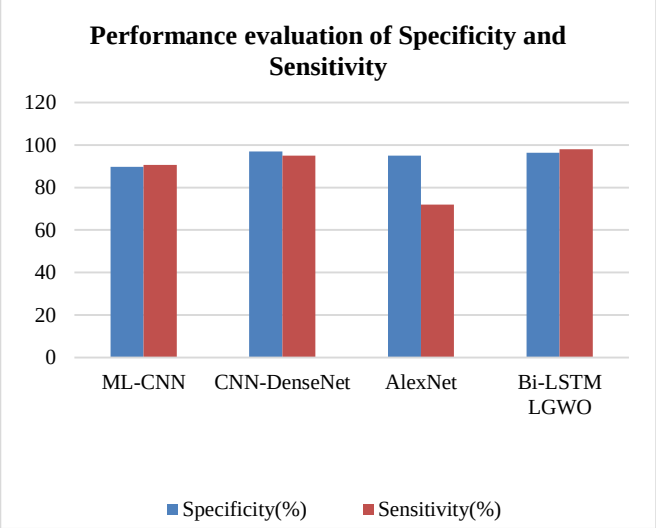

Fig. 5. Comparison of sensitivity and specificity for existing and proposed methods.

Comparison of the proposed model performance results with the existing methods is mentioned in Table II. For clear understanding comparative analysis of sensitivity and specificity are graphically represented in Fig. 5.

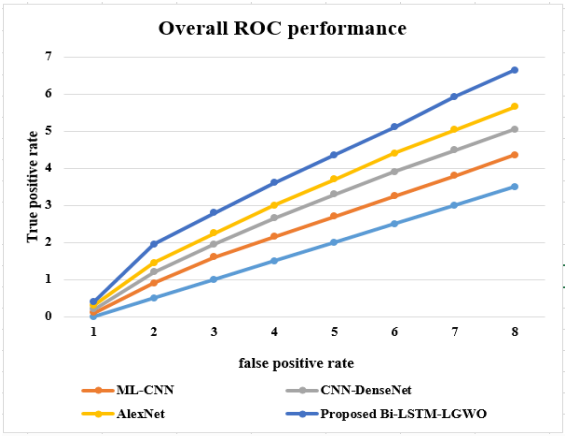

Fig. 6. ROC comparison.

Fig. 6 displays the ROC curve for different models used in ovarian cancer detection. The x-axis represents the FPR, and the y-axis represents the TPR. The proposed Bi-LSTM-LGWO model achieves the highest TPR of 0.7, outperforming ML-CNN, CNN-DenseNet, and AlexNet, which have TPR values of 0.4 and 0.3.

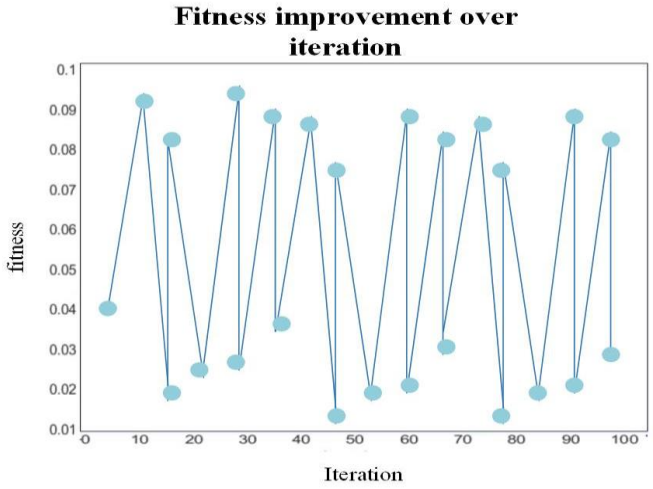

Fig. 7. Fitness improvement.

Fig. 7 shows optimization, fitness improvement refers to the enhancement of the objective function's value or performance metric being optimized. This can be achieved by applying various optimization techniques, such as evolutionary algorithms, gradient descent, or simulated annealing, to iteratively search for better solutions.

B. Discussion

The findings of the suggested Bi-LSTM-LGWO model are highly encouraging, with a great sensitivity of 99.7% and an amazing accuracy of 98%. These results indicate that the model performs very well in detecting ovarian cancer properly, which is essential for early diagnosis and management. However, it's important to recognize that the suggested task has certain limits. First off, as larger and more diverse datasets are frequently needed for reliable performance, this may have an impact on how generalizable the model is. Second, the Bi-LSTM-LGWO model's computational complexity could make it impractical to use in real-time clinical situations. Future research should focus on overcoming these constraints by enlarging the dataset and streamlining the model. The model's credibility and suitability for use in clinical practice would also be further increased by investigating new performance indicators and carrying out external validation on various datasets.

VI. CONCLUSION

The suggested method is more effective than current classifiers and provides a better level of accuracy, making it a potential direction for further study. With accuracy of 98%, recall of 99.7%, precision of 93%, and F1-measure of 98%, the provided model exceeds the existing model. In comparison to the MNN-CNN method, the adopted classifier in the suggested model is more effective. In this approach Bi-LSTM model was employed for classification. The suggested methodology makes a significant addition to the field of ovarian cancer identification and classification overall. The suggested approach will then be examined by running tests on data sets from various sources and industries. Exploring

various topologies, optimization methods, and hyper parameters can improve the Bi-LSTM classifier and LGWO optimization algorithm's performance. In future proposed methods, performance should be validated through larger-scale clinical trials and collaborations with healthcare professionals to assess its reliability and effectiveness in practical medical settings.

REFERENCES

[1] S. Akter et al., "Recent Advances in Ovarian Cancer: Therapeutic Strategies, Potential Biomarkers, and Technological Improvements," Cells, vol. 11, no. 4, p. 650, Feb. 2022, doi: 10.3390/cells11040650.

[2] C. Stewart, C. Ralyea, and S. Lockwood, "Ovarian Cancer: An Integrated Review," Semin. Oncol. Nurs., vol. 35, no. 2, pp. 151–156, Apr. 2019, doi: 10.1016/j.soncn.2019.02.001.

[3] S. Lheureux, C. Gourley, I. Vergote, and A. M. Oza, "Epithelial ovarian cancer," The Lancet, vol. 393, no. 10177, pp. 1240–1253, Mar. 2019, doi: 10.1016/S0140-6736(18)32552-2.

[4] "The diagnostic performance of CA125 for the detection of ovarian and non-ovarian cancer in primary care: A population-based cohort study | PLOS Medicine." https://journals.plos.org/plosmedicine/article?id=10.1371/journal.pmed.1003295 (accessed May 16, 2023).

[5] "8775.00.pdf." Accessed: May 15, 2023. [Online]. Available: https://www.cancer.org/content/dam/CRC/PDF/Public/8775.00.pdf

[6] E. Emmings, S. Mullany, Z. Chang, C. N. Landen, S. Linder, and M. Bazzaro, "Targeting Mitochondria for Treatment of Chemoresistant Ovarian Cancer," Int. J. Mol. Sci., vol. 20, no. 1, p. 229, Jan. 2019, doi: 10.3390/ijms20010229.

[7] A. Chandra et al., "Ovarian cancer: Current status and strategies for improving therapeutic outcomes," Cancer Med., vol. 8, no. 16, pp. 7018–7031, 2019, doi: 10.1002/cam4.2560.

[8] "Sci-Hub | Breast cancer diagnosis using multiple activation deep neural network | 10.1177/1063293X211025105." https://sci-hub.wf/10.1177/1063293X211025105 (accessed May 17, 2023).

[9] J. V. Tembhurne, A. Hazarika, and T. Diwan, "BrC-MCDLM: breast Cancer detection using Multi-Channel deep learning model," Multimed. Tools Appl., vol. 80, no. 21–23, pp. 31647–31670, Sep. 2021, doi: 10.1007/s11042-021-11199-y.

[10] S. K. Rajeev, M. Pallikonda Rajasekaran, G. Vishnuvarthanan, and T. Arunprasath, "A biologically-inspired hybrid deep learning approach for brain tumor classification from magnetic resonance imaging using improved gabor wavelet transform and Elmann-BiLSTM network," Biomed. Signal Process. Control, vol. 78, p. 103949, Sep. 2022, doi: 10.1016/j.bspc.2022.103949.

[11] S. Srivastava, P. Kumar, V. Chaudhry, and A. Singh, "Detection of Ovarian Cyst in Ultrasound Images Using Fine-Tuned VGG-16 Deep Learning Network," SN Comput. Sci., vol. 1, no. 2, p. 81, Mar. 2020, doi: 10.1007/s42979-020-0109-6.

[12] X. Meng, X. Li, and X. Wang, "A Computationally Virtual Histological Staining Method to Ovarian Cancer Tissue by Deep Generative Adversarial Networks," Comput. Math. Methods Med., vol. 2021, pp. 1–12, Jul. 2021, doi: 10.1155/2021/4244157.

[13] Z. Fan et al., "Using machine learning to predict ovarian cancer," Int. J. Med. Inf., vol. 141, p. 104195, Sep. 2020, doi: 10.1016/j.ijmedinf.2020.104195.

[14] D. Schwartz, T. W. Sawyer, N. Thurston, J. Barton, and G. Ditzler, "Ovarian cancer detection using optical coherence tomography and convolutional neural networks," Neural Comput. Appl., vol. 34, no. 11, pp. 8977–8987, Jun. 2022, doi: 10.1007/s00521-022-06920-3.

[15] J. Yang, C. Xiang, and J. Liu, "Clinical significance of combining salivary mRNAs and carcinoembryonic antigen for ovarian cancer detection," Scand. J. Clin. Lab. Invest., vol. 81, no. 1, pp. 39–45, Feb. 2021, doi: 10.1080/00365513.2020.1852478.

[16] Z. Zhang and Y. Han, "Detection of Ovarian Tumors in Obstetric Ultrasound Imaging Using Logistic Regression Classifier With an Advanced Machine Learning Approach," IEEE Access, vol. 8, pp. 44999–45008, 2020, doi: 10.1109/ACCESS.2020.2977962.

[17] J. D. Kaggie et al., "Feasibility of Quantitative Magnetic Resonance Fingerprinting in Ovarian Tumors for T 1 and T 2 Mapping in a PET/MR Setting," IEEE Trans. Radiat. Plasma Med. Sci., vol. 3, no. 4, pp. 509–515, Jul. 2019, doi: 10.1109/TRPMS.2019.2905366.

[18] S. Negi, P. Mittal, and B. Kumar, "Modeling and Analysis of High-Performance Triple Hole Block Layer Organic LED Based Light Sensor for Detection of Ovarian Cancer," IEEE Trans. Circuits Syst. Regul. Pap., vol. 68, no. 8, pp. 3254–3264, Aug. 2021, doi: 10.1109/TCSI.2021.3078510.

[19] K. Kasture, "OvarianCancer&Subtypes." Mendeley, Mar. 31, 2021. doi: 10.17632/W39ZGKSP6N.1.

[20] "Automatic Detection and Segmentation of Ovarian Cancer Using a Multitask Model in Pelvic CT Images." https://www.hindawi.com/journals/omcl/2022/6009107/ (accessed May 18, 2023).

[21] X. Wang et al., "Intelligent Hybrid Deep Learning Model for Breast Cancer Detection," Electronics, vol. 11, no. 17, Art. no. 17, Jan. 2022, doi: 10.3390/electronics11172767.

[22] K. Srilatha and V. Ulagamuthalvi, "Support Vector Machine And Particle Swarm Optimization Based Classification Of Ovarian Tumour," Biosci. Biotechnol. Res. Commun., vol. 12, no. 3, pp. 714–719, Sep. 2019, doi: 10.21786/bbrc/12.3/24.

[23] N. Dhanachandra and Y. J. Chanu, "An image segmentation approach based on fuzzy c-means and dynamic particle swarm optimization algorithm," Multimed. Tools Appl., vol. 79, no. 25–26, pp. 18839–18858, Jul. 2020, doi: 10.1007/s11042-020-08699-8.

[24] C.-L. Huang, M.-J. Lian, Y.-H. Wu, W.-M. Chen, and W.-T. Chiu, "Identification of Human Ovarian Adenocarcinoma Cells with Cisplatin-Resistance by Feature Extraction of Gray Level Co-Occurrence Matrix Using Optical Images," Diagnostics, vol. 10, no. 6, Art. no. 6, Jun. 2020, doi: 10.3390/diagnostics10060389.

[25] L. K. Kumari and B. N. Jagadesh, "A Robust Feature Extraction Technique for Breast Cancer Detection using Digital Mammograms based on Advanced GLCM Approach," EAI Endorsed Trans. Pervasive Health Technol., vol. 8, no. 30, pp. e3–e3, Jan. 2022, doi: 10.4108/eai.11-1-2022.172813.

[26] Q. M. Alzubi, M. Anbar, Z. N. M. Alqattan, M. A. Al-Betar, and R. Abdullah, "Intrusion detection system based on a modified binary grey wolf optimisation," Neural Comput. Appl., vol. 32, no. 10, pp. 6125–6137, May 2020, doi: 10.1007/s00521-019-04103-1.

[27] V. A. Chinnasamy and D. R. Shashikumar, "Breast cancer detection in mammogram image with segmentation of tumour region," Int. J. Med. Eng. Inform., vol. 12, no. 1, pp. 77–94, Jan. 2020, doi: 10.1504/IJMEI.2020.105658.

[28] R. Yazdani, M. Mirmozaffari, E. Shadkam, and M. Taleghani, "Minimizing total absolute deviation of job completion times on a single machine with maintenance activities using a Lion Optimization Algorithm," Sustain. Oper. Comput., vol. 3, pp. 10–16, Jan. 2022, doi: 10.1016/j.susoc.2021.08.003.

[29] V. A. Chinnasamy and D. R. Shashikumar, "Breast cancer detection in mammogram image with segmentation of tumour region," Int. J. Med. Eng. Inform., vol. 12, no. 1, pp. 77–94, 2020.

[30] P. H. Nagarajan and N. Tajunisha, "Optimal Parameter Selection-based Deep Semi-Supervised Generative Learning and CNN for Ovarian Cancer Classification," ICTACT J. SOFT Comput., vol. 13, no. 02, 2023.

[31] H. Su, E. Zio, J. Zhang, M. Xu, X. Li, and Z. Zhang, "A hybrid hourly natural gas demand forecasting method based on the integration of wavelet transform and enhanced Deep-RNN model," Energy, vol. 178, pp. 585–597, Jul. 2019, doi: 10.1016/j.energy.2019.04.167.

[32] S. Bhanumathi and S. N. Chandrashekara, "DEEP EARNING BASED BiLSTM ARCHITECTURE FOR LUNG CANCER CLASSIFICATION," Int. J. Adv. Res. Eng. Technol. IJARET, vol. 12, no. 1, pp. 492–503, 2021.

[33] B. Jang, M. Kim, G. Harerimana, S. Kang, and J. W. Kim, "Bi-LSTM Model to Increase Accuracy in Text Classification: Combining

Word2vec CNN and Attention Mechanism," Appl. Sci., vol. 10, no. 17, p. 5841, Aug. 2020, doi: 10.3390/app10175841.

[34] Z. Zhang and Y. Han, "Detection of ovarian tumors in obstetric ultrasound imaging using logistic regression classifier with an advanced machine learning approach," IEEE Access, vol. 8, pp. 44999–45008, 2020.

[35] G. Wadhwa, "A Deep Convolutional Neural Network Approach for Detecting Malignancy of Ovarian Cancer Using Densenet Model," vol. 25, no. 2, 2021.

[36] K. R. Kasture and E. Al, "A New Deep Learning method for Automatic Ovarian Cancer Prediction & Subtype classification," Turk. J. Comput. Math. Educ. TURCOMAT, vol. 12, no. 12, Art. no. 12, May 2021.